24th COBEM - 2017

24th ABCM International Congress of Mechanical Engineering
December 3-8, 2017, Curitiba, PR, Brazil

COBEM-2017-2376
COMPENSATION OF THE ENGINE INDICATING PRESSURE SIGNAL DISTORTION PRODUCED BY A FIBER-OPTIC SENSOR

Dinarte Santos
Petrobras - REFAP, Brazil
Federal University of Technology - Parana, Department of Mechanical Engineering, Brazil
dinarte47@yahoo.com.br

Irionson Antônio Bassani
Pontifical Catholic University of Parana, Department of Mechanical Engineering, Brazil
irionson.bassani@pucpr.br

José Antonio Velásquez
Federal University of Technology - Parana, Department of Mechanical Engineering, Brazill
velasquez@utfpr.edu.br

Abstract. *This article describes the development of a procedure that allows compensating the signal distortion of the in-cylinder pressure, as measured with a fiber-optic pressure sensor. The corrective procedure is based on a comparison of experimental pressure data with the corresponding simulated results given by a thermodynamic model, which allows calculating the working cycle of a spark ignition engine, including the compression, combustion-expansion, as well as the exhaust and intake processes. This computational model takes into account the finite duration of the combustion process, the heat transfer between the working fluid and cylinder walls, and the mass flow through the intake and exhaust valves. Additionally, the correlation proposed by Wiebe was used to represent the combustion heat release. The model was initially applied for simulating the motored operation of a single-cylinder, variable compression-ratio CFR engine. Afterwards, results of this simulation as well as experimental data were used to calculate the parameters of a second order high-pass filter model, which was used to represent the behavior of the fiber-optic pressure sensor. Corrected in-cylinder pressure data measured on the CFR engine during its fired operation were, then, employed in order to validate the data treatment procedure.*

Keywords: *Compensation of measurement signal distortion; Fiber-optic pressure sensor; Engine indicating measurements; Two-zone combustion model; Variable compression ratio CFR engine.*

1. INTRODUCTION

Engine indicating includes the measurement of instantaneous in-cylinder pressure, the determination of the top dead centre (TDC) and the measurement of the instantaneous crank angle. These measurements are fundamental for engine combustion diagnosis and for indicated work calculation. In engine combustion diagnosis, the apparent heat release rate and the combustion reaction extent are the most useful quantities obtainable from engine indicating data (Bueno *et al*., 2012). The apparent heat release rate is calculated by computing the amount of fuel chemical energy release necessary to obtain the experimentally observed pressure, while the combustion reaction extent is evaluated through the released fraction of the total fuel chemical energy. Heat release analysis is often complemented using optical techniques and its utilization as a diagnostic tool covers a wide range of objectives, including the development of new combustion systems, the analysis of the performance of a newly formulated fuel, the validation of mathematical models for engine simulation and the study of new strategies for fuel supplying into the engine.

The analysis of the processes occurring in the cylinder of internal combustion engines requires pressure transducers with high specifications regarding linearity, frequency response and resistance to thermal solicitations. Studies comparing transducers available at the end of 1960 decade (see for example Brown, 1967) found that those having piezoelectric crystals as measuring elements exhibited better tolerance to thermal solicitations than those based on strain gauges. By this reason, piezoelectric transducers eventually spread to measure the in-cylinder pressure, while sensors based on strain gauges (metal or piezo-resistive) were preferably used in measurements where the thermal solicitations are modest, such as pressure measuring in the fuel injection line and in the intake manifold. However, although

piezoelectric transducers are capable of maintaining high characteristics in frequency response and linearity over a wide range of pressures, drawbacks related to instability of the baseline, low intensity of output signal, high electromagnetic interference and, mainly, the fact that they are unacceptably expensive are frequently claimed. This way, their use in production engines is considered prohibitive.

In contrast, fiber-optic pressure sensors exhibit very low cost, thus becoming prime candidates for use in automotive production engines (Wlodarczyk *et al*., 1998). Due to its reduced dimensions, these sensors can be combined with existing engine components such as ignition spark plugs, fuel injectors, or glow plugs in order to minimize total installation and operational cost. Such an embedded sensor does not require a separate access point into the engine and the device that the sensor is integrated with can be conventionally installed. No additional cable or connector is needed since the pressure sensor information is sent via the existing cable and connector (Wlodarczyk, 2000).

In the present work a fiber-optic pressure sensor Optrand D312A8-QA was used for engine indicating and a signal treatment procedure was developed in order to compensate the distortion stemming from its reduced frequency response.

2. DEVELOPMENT OF THE SIMULATION MODEL

A mathematical model was developed from mass and energy conservation principles written for the control volume shown in Fig. 1. The model development methodology was based on the work authored by Stiesch (2006) and follows these steps:

- Definition of the system (through the identification of its boundaries) and determination of both the relevant surroundings as well as the mass and energy interactions between the system and surroundings;
- Mass and energy accounting for the system;
- Description of the mass and energy flows, based on physical laws;
- Model simplification, neglecting secondary influences;
- Numerical integration of the differential equation set;
- Plotting the *p*-*V* diagram from the complete cycle simulation results;
- Validation of the model by comparing simulated results with experimental data.

A four-stroke engine cycle comprises admission, compression, expansion, and exhaust. Combustion takes place during the final part of the compression and the initial part of the expansion strokes. In order to represent this process, a two zone thermodynamic model was used, while for the rest of the cycle a single zone model was employed. These models consist of a set of differential equations based on the laws of mass and energy conservation and on the ideal gases law. When developing the mathematical model, calculation procedures for the following aspects were included: (*i*) Thermodynamic properties of the working fluid (unburned and burned gases); (*ii*) Equilibrium composition of the combustion products; (*iii*) Rate of heat transfer to the cylinder walls; (*iv*) Fuel burning rate, as described by the Wiebe correlation. In order to simplify the calculation of the combustion products composition, the number of chemical species present therein was limited to twelve, namely H, He, N, H_2, OH, CO, NO, O_2, H_2O, CO_2, N_2, Ar; and it was considered that these species are in full thermodynamic equilibrium (Olikara and Borman, 1975). Consequently, the effects of temperature gradients, pressure waves, non-equilibrium compositions, fuel atomization and vaporization are all ignored (Krieger and Borman, 1966).

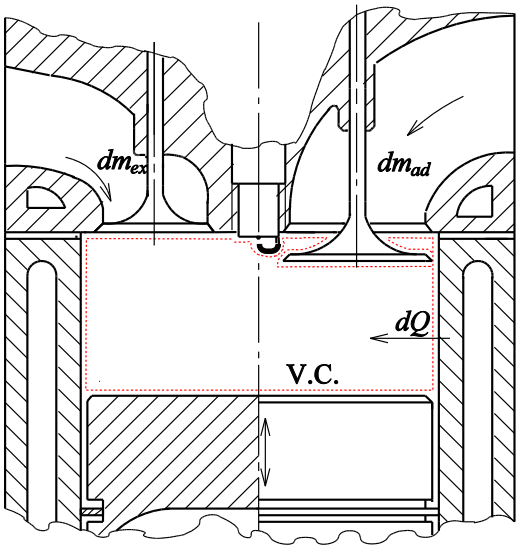

Figure 1. Control volume for in-cylinder processes analysis.

The heat transfer rate between the gases and cylinder walls is assumed uniform across each of the wall surfaces (Annand, 1963) and was computed as the product of the instantaneous cylinder area, the instantaneous temperature difference between the gases and walls, and the convection coefficient. The instantaneous area of the cylinder walls was calculated from their geometry and from the kinematics of the crank-rod mechanism, assuming that the crankshaft angular speed ω is constant and neglecting the effects of torsional vibrations due to both the engine torque pulsing character and the flywheel finite moment of inertia. This allows determining the angular position of the crankshaft $\theta(t)$ through the expression $\theta(t) = \omega \cdot t$ instead of using Eq. (1), which allows for an additional simplification of the model.

$$\theta(t) = \int \omega \cdot dt \tag{1}$$

The convection coefficient was computed from Woschni's formula, which is an empirical function of cylinder geometric parameters and piston average speed (Woschni, 1967). Additionally, fuel burning rate was computed by Wiebe's formula, an empirical correlation with three adjustable parameters, which avoids the need for computing flame area and volume, thus further simplifying the mathematical model (Heywood, 1989). Specific enthalpy, specific internal energy and specific heats of each chemical species present in the working fluids were computed by Shomate's polynomials (Linstrom and Mallard, 2015).

The cylinder head, piston and valves are assumed all rigid, neglecting any deformations caused by inertial forces, pressure, or thermal expansion. The cylinder volume displacements due to valve stem movements are considered negligible. This hypothesis is justified because during the compression and expansion times the valves are closed, therefore immobile, and during the inlet and exhaust strokes, when they are open, the cylinder pressure variations are small. Thus, the effects of any moving parts deflections or valve movements on the volume of the cylinder are neglected. These hypotheses allow the determination of cylinder areas and volumes, depending only on geometric parameters of the cylinder and kinematic parameters of crank-rod mechanism. Both the gaskets and the valves are assumed perfect sealants, i.e., zero gas leakage or blow-by through the ring gaps, piston and cylinder wall clearance, or valve seating surfaces is assumed. Therefore, the mass of the gases inside the cylinder gases can be assumed constant, as long as the inlet and exhaust valves are both closed.

The above assumptions lead to a model describing the rates of change of the in-cylinder pressure (dp/dt) as well as of the temperatures of unburned and burned zones (dT_u/dt and dT_b/dt):

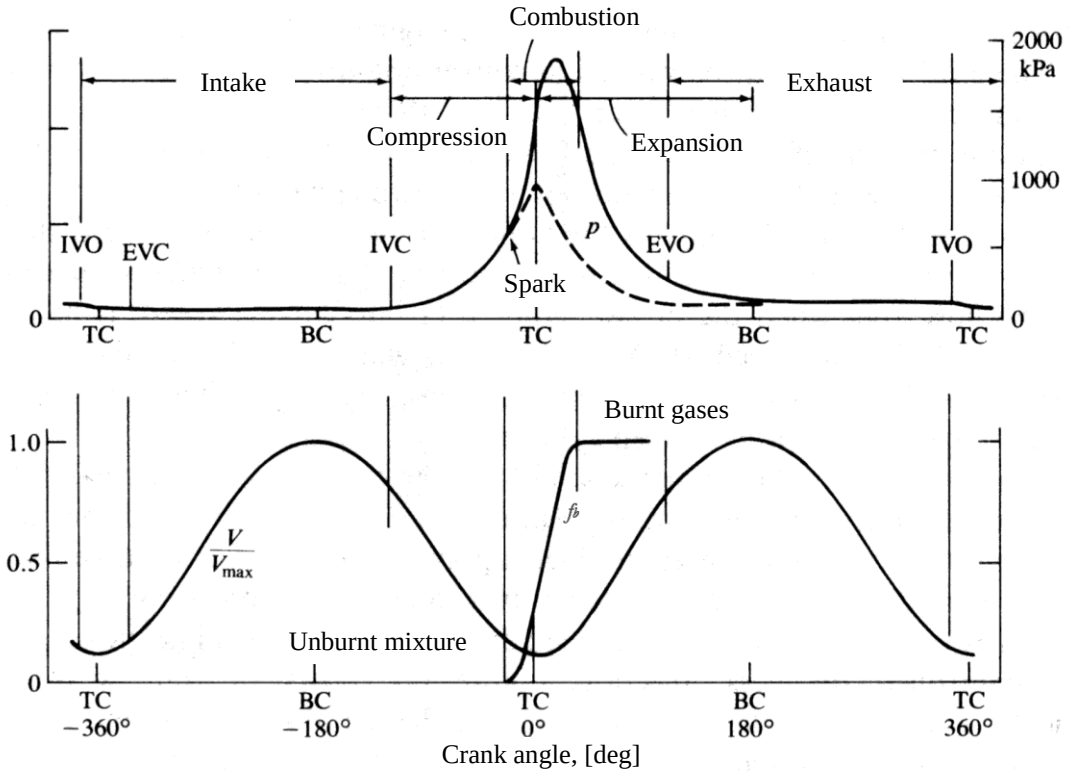

Figure 2: Pressure, volume and burnt mass fraction profiles as a function of crank angle (Heywood, 1988).

$$A \cdot \begin{bmatrix} dp/dt \\ dT_u/dt \\ dT_b/dt \end{bmatrix} = B \tag{2}$$

where A is a third order square matrix whose elements are functions of the cylinder gases thermodynamic state, while B is a column vector whose elements are functions of the rate of heat transfer to cylinder walls, of the rate of cylinder volume change and of the combustion burning rate. Numerical integration of dp/dt, dT_u/dt and dT_b/dt requires initial values of in-cylinder pressure and temperature. Figure 2 shows the pressure, volume and burned mass fraction profiles, as a function of the crankshaft angular position.

3. RESULTS AND DISCUSSION

Intake and exhaust valve discharge coefficients were measured in a flow bench and a polynomial function was fitted to experimental data. These polynomials were used in the computational model in order to obtain intake and exhaust mass flow rates. Valve lift curves were measured while turning the engine crankshaft by hand, and a Fourier series was fitted to represent these curves. Both the Fourier series and the polynomial function were used in the simulation model to compute mass flow through the valves. In addition, experimental pressure curves and classic $p-V$ diagrams were obtained for the Waukesha CFR engine under both motored and fired working conditions. In order to measure in-cylinder pressure, a fiber-optic pressure sensor Optrand D312A8-QA and a digital storage oscilloscope were used.

Figure 3 compares raw pressure experimental data with simulation results. As can be seen in this figure, the experimental pressure data profile differs significantly from the simulation results. Throughout the intake stroke, the experimental pressure is higher than during the exhaust stroke. In this way the air would flow against the differential pressure, which has no physical realism. The pressure inside the cylinder should be slightly below atmospheric during the intake stroke to allow the air entering into it. In addition, the data plot shows a hysteresis loop during the compression and expansion strokes. This loop would be possible if there were a strong heat exchange between the air and the cylinder walls, or a systematic error in readings of the crankshaft angular position, or even in the case of a the pressure sensor signal distortion. The air to wall heat transfer coefficient is not high (Woschni, 1967), which rules out the first possibility. A systematic error in the readings of the crankshaft angular position was discarded after checking it with a stroboscopic timing light. Thus, the disagreement is mostly due to pressure sensor response low frequency limitation, and the experimental pressure data must be corrected before compared with the simulation results.

There was no instrument available to measure the pressure sensor frequency response, which could be inverted to compensate the experimental raw data distortion, so the alternative procedure of fitting experimental data to simulation

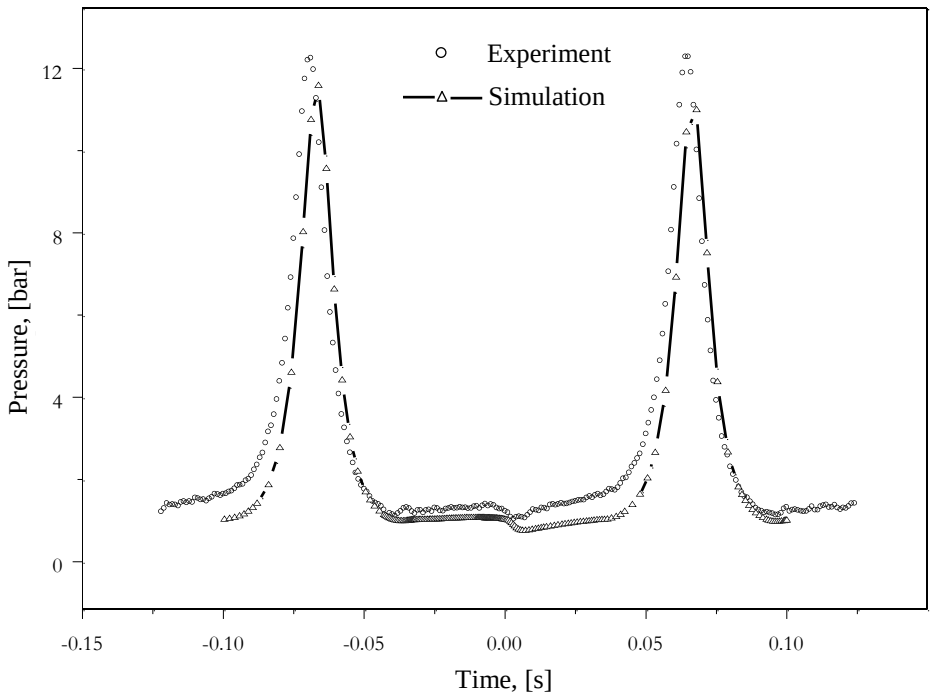

Figure 3: Comparison between raw experimental pressure data and simulation results.

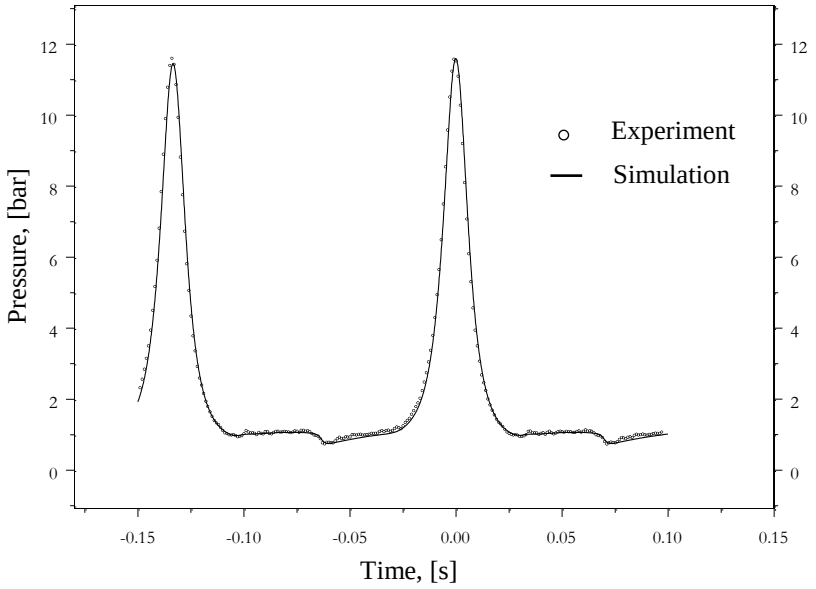

Figure 4: Comparison of simulation results with experimental data after signal treatment (motored engine).

results was used. The parameters of a parametric physical model describing the sensor frequency response were adjusted to minimize the sum of the squared differences between the simulation results and the experimental data. A second order, high-pass filter model was adopted, which had as its parameters the pressure sensor damping coefficient, natural frequency, sensitivity and zero. The filter output provided the Fourier transform coefficients of the corrected pressure data and the corrected experimental pressure data were obtained by applying the inverse Fourier transform to these coefficients. These corrected data were then compared with the results of the simulation and the sum of the quadratic differences was minimized using Newton's method. This way, the damping coefficient, natural frequency, sensitivity and zero parameters in the sensor's physical model were determined.

Figure 4 compares the simulation results with corrected experimental pressure data, as functions of time, while Figure 5 shows a *p*-*V* diagram plotted from simulated and corrected experimental data. As can be seen in these figures, there are no significant differences and the quality of fitting is evident.

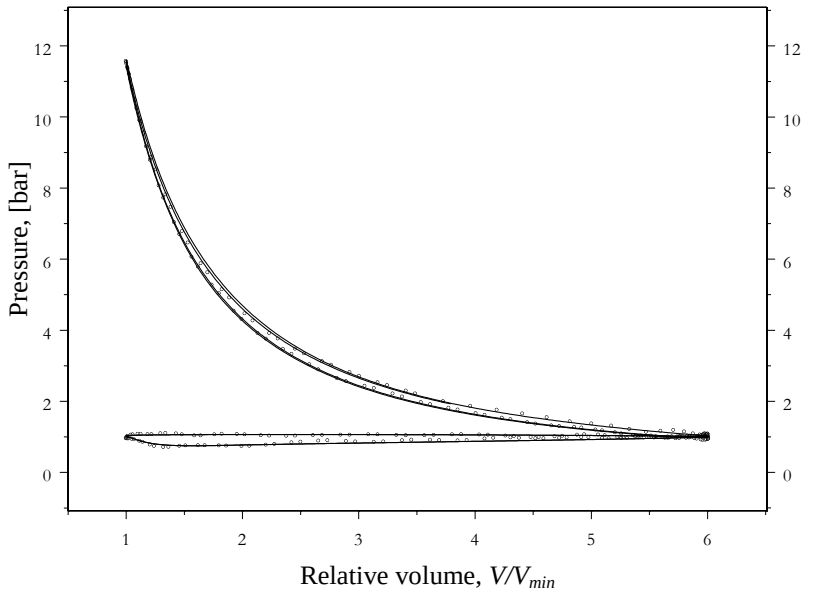

Figure 5. Comparison of simulated and compensated experimental data (motored CFR engine, 6:1 compression ratio).

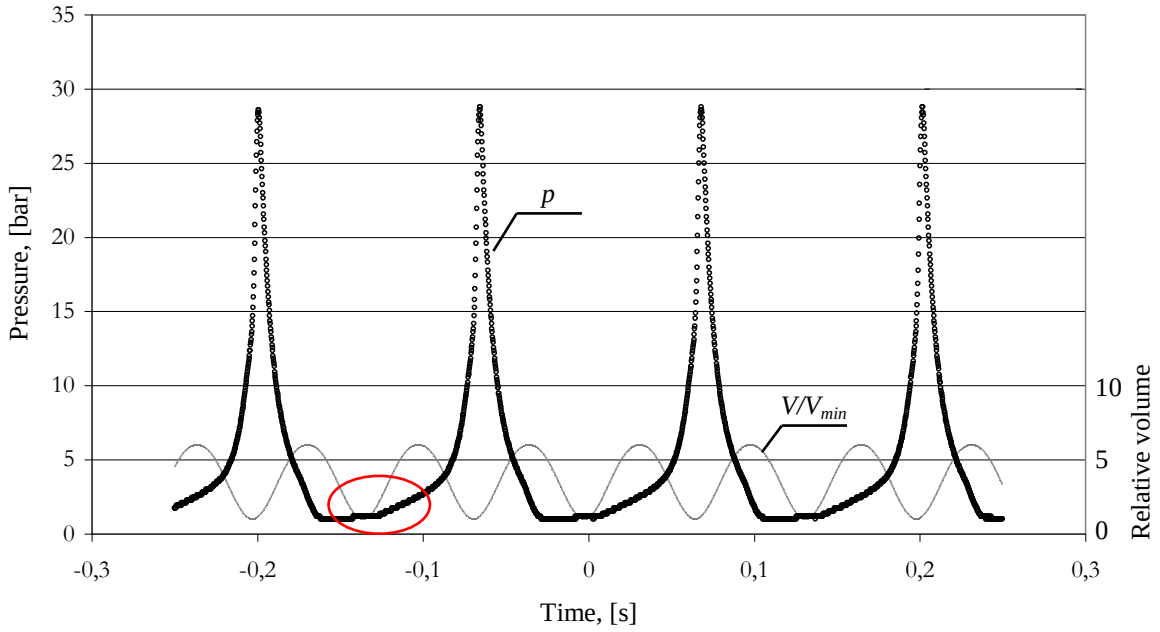

The in-cylinder pressure and volume data were measured under fired operation with the CFR engine fueled by a stoichiometric mixture of isooctane and atmospheric air. Figure 6 shows the measured raw data. It can be seen in this figure that pressure behavior looks as is typical for an internal combustion engine. During compression, when intake and exhaust valves are closed, pressure rises while volume is being reduced. After the beginning of combustion the cylinder pressure reaches a peak value and then falls as expansion takes place. Pressure peak values as well as the rates of pressure rising and falling are higher than under motored operation conditions (shown in Fig. 3). However, as it can be noted in the region highlighted with a red ellipse, during the initial stage of the intake stroke the in-cylinder pressure is greater than in the final stage of the exhaust process, which is inconsistent with the expected behavior, thus revealing the distortion of the measured pressure signal.

Figure 6: Raw experimental pressure and relative cylinder volume data as functions of time.

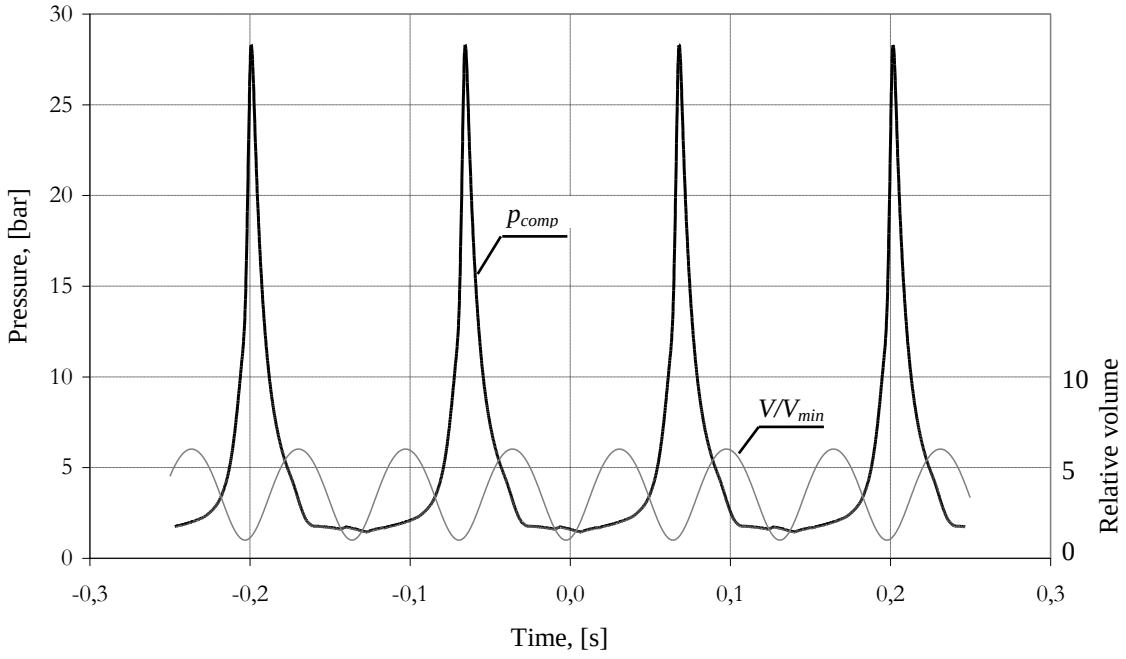

Figure 7: Compensated experimental pressure and relative volume profiles.

Figure 7 shows both compensated experimental pressure data and relative cylinder volume as functions of time. Compensation affects mostly the experimental pressure data during the intake, as well as at the end of the expansion and exhaust strokes. Figure 8 shows the validation of the corrective procedure by comparing simulation results with experimental data averaged over 128 engine cycles, along four complete simulated engine cycles. The cylinder pressure is higher throughout the first than in the remaining cycles, because there are no residual gases in the cylinder at the start of engine operation. From the second simulated cycle on, both profiles nearly overlap.

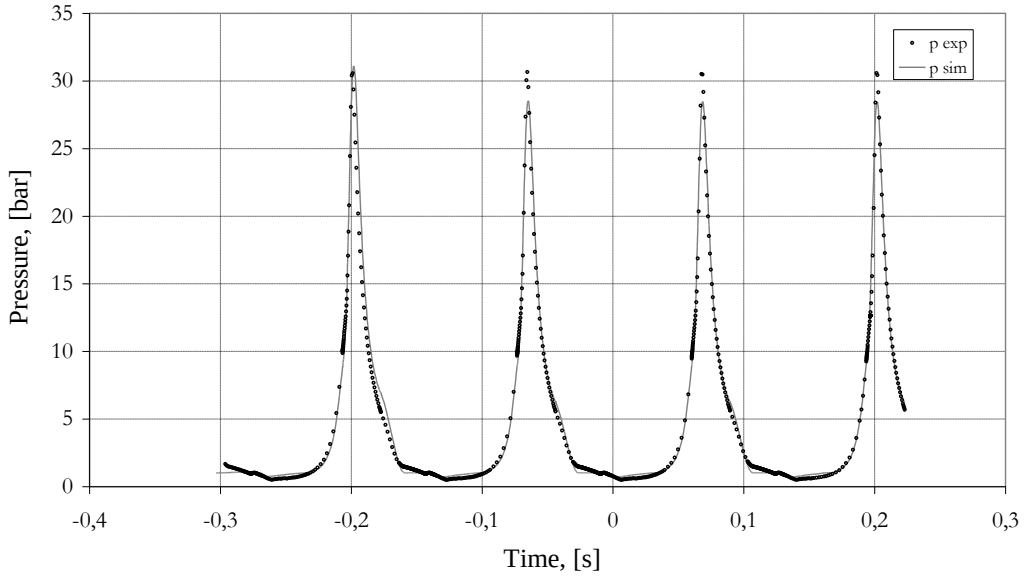

Figure 8: Comparison between simulation results and compensated experimental cylinder pressure data.

Figure 9 shows the *p-V* diagram for the operation under fired conditions. The internal area of the first simulated cycle area is larger than the areas of the subsequent ones. This is due to the absence of residual gases at the beginning of the simulation. From the second cycle on, the simulation results nearly overlap the experimental data.

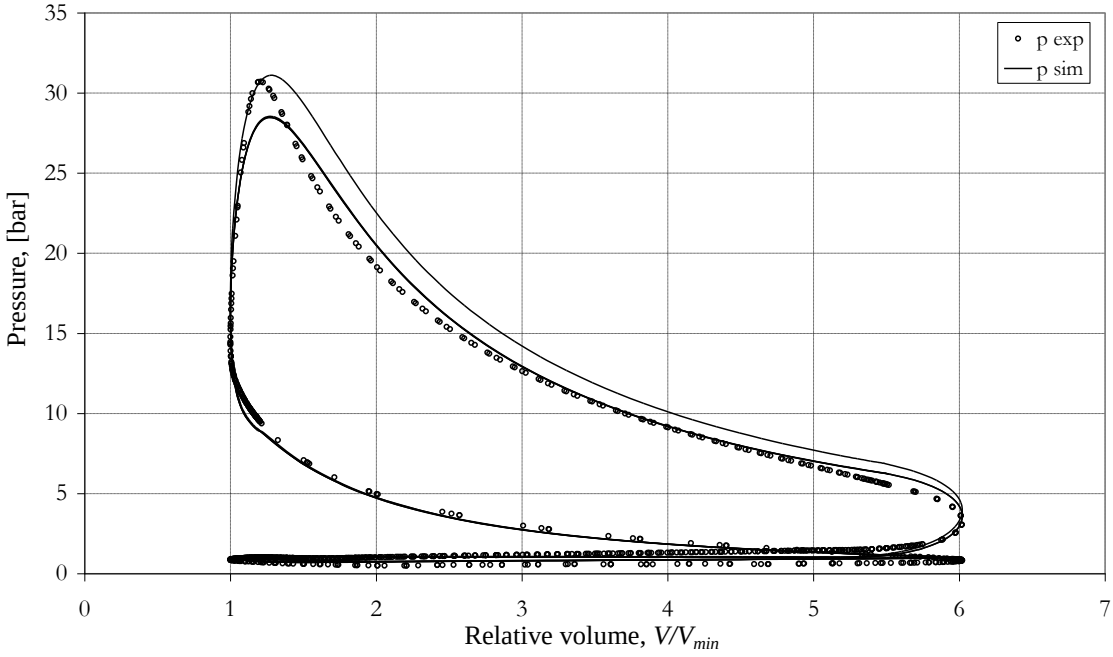

Figure 9: CFR engine *p-V* diagram.

The agreement between the diagrams is good over most of the cycle, roughly validating the thermodynamic model. The simulation model reproduces the experimental data accurately along the exhaust process (starting from the bottom dead center - BDC) as well as along the intake and the compression strokes (until ignition takes place). This confirms that the compensation of the sensor frequency response was able to make these processes of the simulated and experimental *p-V* diagrams overlap and that the single zone exhaust, intake and compression model is accurate. However, experimental pressure data and simulated results differ during the combustion process. The experimental pressure data begin to rise sooner after ignition, reaches a higher peak and decreases faster than the simulation results. As the sensor frequency compensation was not able to make the experimental and simulated diagrams agree during the combustion section but elsewhere the compensation was effective, the possibility of error due to faulty sensor compensation is discarded, and the possibility of error introduced by inaccurate combustion model parameters remains to be analyzed.

4. CONCLUSIONS

A two-zone combustion model was developed to represent the CFR engine cycle and experimental pressure data were collected on this engine under motored and fired operation. It was found that the experimental raw data needed a treatment to compensate for errors due to frequency response distortion inherent to the pressure sensor, which acted as a high-pass filter. Then, experimental data were treated for noise reduction and a correction procedure was developed. This correction procedure consisted of applying a second order inverse response filter in the frequency domain to the Fourier transform coefficients a_i and b_i, which were obtained by applying the Fourier transform to the digitally acquired pressure data. After correction, the simulation results were found to be in good agreement with the experimental data. However, fitting quality was better for motored than for fired operation conditions. Further work is needed to improve determination of filter parameters model that allow better fitting for fired operation conditions.

5. REFERENCES

Annand W. J. D. (1963). “Heat transfer in cylinders of reciprocating internal combustion engines”. *Proceedings of the Institution of Mechanical Engineers*, 177(36) pp. 973-990.

Brown W. L. (1967). “Methods for evaluating requirements and errors in cylinder pressure measurement”. *SAE Paper 670008*.

Bueno A. V., Velásquez J. A. and Milanez L. F. (2012). “Internal Combustion Engine Indicating Measurements”. In: Haq Z. (Ed.), *Applied Measurement Systems*, InTech, DOI: 10.5772/37889. Available from: https://www.intechopen.com/books/applied-measurement-systems/internal-combustion-engine-indicating-measurements

Heywood J. B. (1989). *Internal Combustion Engine Fundamentals*. McGraw-Hill, New York.

Krieger R. B. and Borman G. L. (1966). “The computation of apparent heat release for internal combustion engines”. *ASME paper 66-WA/DGP-4*.

Linstrom P. J. and Mallard W. G. (2015). *NIST Chemistry WebBook, NIST Standard Reference Database Number 69*. National Institute of Standards and Technology, Gaithersburg MD, 20899, doi:10.18434/T4D303, (accessed in July, 2015).

Olikara C. and Borman G. L. (1975). “A computer program for calculating properties of equilibrium combustion products with some applications to I. C. engines”. *SAE paper 750468*.

Stiesch, G. (2006). *Simulating Combustion*. Springer, Berlin.

Wlodarczyk M. T. (2000). “Long-life fiber-optic pressure sensors for control and monitoring of combustion engines”. In: Krüger S., Gessner W. (Eds.), *Advanced Microsystems for Automotive Applications*. VDI-Buch. Springer, Berlin, Heidelberg.

Wlodarczyk M.T., Poorman T., Xia L., Arnold J. and Coleman T. (1998). “In-cylinder fiber-optic pressure sensors for monitoring and control of diesel engines”. *SAE Technical Paper 981913*. https://doi.org/10.4271/981913

Woschni G. (1967). “A universally applicable equation for the instantaneous heat transfer coefficient in the internal combustion engine”. *SAE Transactions 670931*, pp. 3065-3082.

6. RESPONSIBILITY NOTICE

The authors are the only responsible for the printed material included in this paper.